Talanta 100 (2012) 282–289

Contents lists available at SciVerse ScienceDirect

Talanta

journal homepage: www.elsevier.com/locate/talanta

# Graphene-carbon paste electrode for cadmium and lead ion monitoring in a flow-based system

Wanida Wonsawat [a], Suchada Chuanuwatanakul [a,b], Wijitar Dungchai [c], Eakkasit Punrat [a], Shoji Motomizu [d], Orawon Chailapakul [a,b,*]

[a] Electrochemistry and Optical Spectroscopy Research Unit, Department of Chemistry, Faculty of Science, Chulalongkorn University, 254 Phayathai Road, Pathumwan, Bangkok 10330, Thailand
[b] Center of Excellence for Petroleum, Petrochemicals and Advanced Materials, Chulalongkorn University, 254 Phayathai Road, Pathumwan, Bangkok 10330, Thailand
[c] Department of Chemistry, Faculty of Science, King Mongkut's University of Technology Thonburi, 126 Prachautid Road, Thungkru, Bangkok 10140, Thailand
[d] Department of Chemistry, Faculty of Science, Okayama University, Tsushimanaka 3-1-1, Okayama 700-8530, Japan

ARTICLE INFO

*Article history:*
Received 27 February 2012
Received in revised form
16 July 2012
Accepted 16 July 2012
Available online 22 July 2012

*Keywords:*
Graphene modified electrode
Carbon paste electrode
Lead
Cadmium
Sequential injection analysis

ABSTRACT

An environment friendly electrode for determining $Cd^{2+}$ and $Pb^{2+}$ levels in an automated flow system was successfully developed. Cyclic voltammetry and square wave anodic stripping voltammetry (SWASV) coupled with sequential injection analysis (SIA) were employed to study the electrochemical behavior of the electrode. The *in situ* bismuth-modified graphene-carbon paste electrode (Bi-GCPE) exhibited excellent electrooxidation of $Cd^{2+}$ and $Pb^{2+}$ in the automated flow system with a significantly higher peak current for both metal ions compared with the unmodified CPE. The limits of detection from this method were 0.07 and 0.04 μg $L^{-1}$ for $Cd^{2+}$ and $Pb^{2+}$, respectively, with a linear oxidation peak current response for $Cd^{2+}$ and $Pb^{2+}$ in the range of 0.10–50.0 μg $L^{-1}$ under optimum conditions. The Bi-GCPE was also applied for the determination of $Cd^{2+}$ and $Pb^{2+}$ in low- (tap water) and high- (sea bass fish and undulated surf clam tissues) matrix complexity samples by automated flow system. The recoveries were acceptable and ranged from 70.4% to 120% for $Cd^{2+}$ and 65.8% to 113.5% for $Pb^{2+}$.



## 1. Introduction

Graphene, a new class of promising carbon material, is of great interest. Graphene is a two-dimensional (2D) material that is composed of a planar monolayer of $sp^2$ carbon atoms bonding in a hexagonal configuration [1]. The unit cell of graphene contains two carbon atoms with an inter-atomic length of 0.142 nm. In addition, it exhibits good electrical conductivity and optical properties, is lightweight, and has a large specific surface area and chemical stability. Because of these properties, a widespread range of novel materials and applications [2,3] have already been generated in various fields, including biomedical sensors, nanoelectronic devices, transparent electrodes, photodetectors, hydrogen storage, solar cells, fuel cells, electrical batteries [4–8] and supercapacitors [9]. Furthermore, compared to carbon nanotubes (CNTs), graphene provides the advantages of low cost and low metallic contamination levels [10,11]. Therefore, graphene has begun to be exploited as an alternative choice for electrical sensors, especially during the fabrication of electrochemical-sensing devices [12]. The first graphene-based electrochemical sensor was reported by Papakonstantinou and co-workers [13]. To improve the sensitivity, the use of metal–graphene nanocomposites, such as with Hg [14], Au [15,16], Co [17], Pd [16,18], Pt [18,19], Ag [18] and Cu [18], has been widely reported. In addition, Wu et al. [20] used a β-cyclodextrin–graphene-modified glassy carbon electrode for the ultra-high sensitive detection of methyl parathion and achieved a limit of detection (LOD) of 0.05 μg $L^{-1}$.

Recently, the analysis of transition heavy metal ions, especially cadmium ($Cd^{2+}$) and lead ($Pb^{2+}$), in the food and environment of humans has gained considerable interest because $Cd^{2+}$ and $Pb^{2+}$ can accumulate in the kidney, liver, lung and central nervous system, allowing sub-toxic exposure levels to accumulate to toxic levels over time [21–23]. They have also been classified as carcinogenic agents by the WHO International Agency for Research on cancer. An increased risk of cancer has been attributed to an increased distribution and concentration of these metal ions in the environment, in terms of exposure time and their concentration levels. Moreover, the long-term exposure to low concentrations of these metals causes adverse health effects.

* Corresponding author at: Electrochemistry and Optical Spectroscopy Research Unit, Department of Chemistry, Faculty of Sciences, Chulalongkorn University, 254 Phayathai Road, Pathumwan, Bangkok 10330, Thailand. Tel.: +66 2 2187615; fax: +66 2 2187309.
*E-mail address:* corawon@chula.ac.th (O. Chailapakul).

0039-9140/$ - see front matter © 2012 Elsevier B.V. All rights reserved.
http://dx.doi.org/10.1016/j.talanta.2012.07.045

Typically, once $Cd^{2+}$ and $Pb^{2+}$ are released into the soil or air, they accumulate in both terrestrial and marine groundwater sources. Although humans might consume the water, it is the bioaccumulation and concentration within the food web, and subsequently the consumption of the contaminated organisms, that is the more serious problem. These organisms can include marine products, such as fish, crabs, crustaceans and seaweeds, as well as freshwater agricultural food products. Thus, a method for the careful monitoring of heavy metals, including $Cd^{2+}$ and $Pb^{2+}$, that is capable of high-throughput applications but is still highly sensitive is a necessary development for on-site screening. Electrochemical methods have been developed for the detection and determination of $Cd^{2+}$ and $Pb^{2+}$ levels because these approaches typically do not require expensive equipment. They also provide high specificity and sensitivity while retaining their simplicity. In recent years, various types of modified electrodes have been developed to overcome the problems of trace metal contamination. Carbon nanotube (CNT)-modified electrodes have been investigated to enhance the signals of target analyte metals. The notable properties of CNTs here are that they increase the electron-transfer kinetics and reduce the overpotential [24,25]. For example, a highly sensitive bismuth (Bi)–Nafion–graphene electrode for the determination of $Cd^{2+}$ and $Pb^{2+}$ levels has been successfully reported by Li et al. [26], with a relatively low LOD of 0.02 $\mu g\,L^{-1}$ for both metal ions. A graphene nanosheet electrode was shown to also have a high sensitivity for $Cd^{2+}$ and $Pb^{2+}$ with LODs of 0.11 and 0.027 $\mu g\,L^{-1}$, respectively, but it was also able to detect $Cu^{2+}$ ions with a LOD of 0.63 $\mu g\,L^{-1}$ [27]. Although these results revealed much lower LODs compared with the results from the CNT-modified electrode, the requirement for the development of flow-automation-compatible electrodes for heavy metal ion detection is still needed to permit the required rapid, flexible, reliable and simultaneous analysis of samples. In this work, sequential injection analysis (SIA) was coupled with a developed graphene electrode because SIA is automatable, fast and simple, and it allows a low reagent consumption and the flexibility to be used in a stopped flow method. To date, only one publication has demonstrated the use of a graphene/Nafion hybrid electrode in a continuous flow system, which is a flow injection-based amperometric glucose biosensor [28]. Therefore, this work reports on the development of the first SIA system that incorporates a graphene electrode for the determination of $Cd^{2+}$ and $Pb^{2+}$.

The *in situ* Bi film combination with the graphene nanocomposite-modified carbon paste electrode (Bi-GCPE) was chosen to simultaneously determine $Cd^{2+}$ and $Pb^{2+}$ levels in an automated SIA system. A wider cathodic potential window, higher overpotential towards the hydrogen evolution reaction, a better long-term stability and reproducibility in the hydrochloric acid (HCl) electrolyte, and a good sensitivity compared to CNT-based electrodes [29–31] were obtained. The fabrication of the Bi-GCPE and optimization of its performance in the SIA system was examined with respect to the simultaneous determination of $Cd^{2+}$ and $Pb^{2+}$ levels.

## 2. Experimental

### 2.1. Instrumentation

The electrochemical measurements were performed using a PalmSens potentiostat (PalmSens BV, The Netherlands). All measurements were performed at room temperature in a transparent in-house flow cell with the test Bi-GCPE (or other test electrode, such as GCPE, CPE or Bi-CPE) as the working electrode, a stainless steel tube counter electrode and an Ag/AgCl (3 mol $L^{-1}$ KCl) reference electrode. A SIA system (MGC auto-Pret MP-014s, MGC, Japan) consisting of an eight-port selection valve, a 2.5 mL syringe pump and 3.0 mL holding coil was used. This system was computer-controlled by the MGC LMPro program ver. 2.5.

### 2.2. Chemicals and reagents

All chemicals and reagents were of analytical reagent grade. Ultrapure water was used to prepare all solutions and was purified by the Milli-Q unit (Millipore, Bedford, USA). Graphene was obtained from SkySpring Nanomaterials (USA). HCl, nitric acid ($HNO_3$), perchloric acid ($HClO_4$) and 2-propanol were purchased from Merck (Merck, Germany). The $Bi^{3+}$, $Cd^{2+}$ and $Pb^{2+}$ solutions were diluted from their respective 1000 mg $L^{-1}$ standard solutions (BDH, England). Graphite powder (particle size $< 20\,\mu m$) and mineral oil were purchased from Sigma-Aldrich.

### 2.3. Graphene dispersion

Commercial graphene nanopowder was used for the preparation of the graphene-carbon paste electrode (GCPE). The graphene-induced aggregation is crucial for the electrochemical signal [32]. Due to the small size and flat shape of graphene, graphene nanopowder is sensitive to van der Waal's interactions and conglomerates in the dry state, leading to poor electrical conductivity [33–35]. Therefore, to obtain the unique and desired properties of graphene-based electrodes, the prevention of graphene aggregation is an important process [36].

A well-dispersed graphene suspension was prepared by ultrasonic dispersing 1 mg graphene in 1 mL of 15% (v/v) isopropanol for 60 min. Next, the dispersed suspension was sonicated for 1 h before graphite powder was added and sonicated for an additional hour, to give a more homogeneously dispersed graphite–graphene suspension. The well-dispersed graphite–graphene suspension was dried by evaporation of solvent in a vacuum oven at 60 °C for 30 min.

### 2.4. Preparation of the GCPEs and CPEs

The GCPEs were prepared by mixing the graphite powder with various amounts of graphene powder and blending this mixture with mineral oil (60%:40% w/w) in an agate mortar to form a homogeneous paste [37,38]. This paste was then filled into the electrode-holder, and a copper wire was inserted into the opposite end for the electrical connector. Prior to use, a fresh and smooth electrode surface was obtained by polishing with weighing paper. The CPEs were prepared by the same procedure without addition of graphene powder. The Bi-GCPEs and Bi-CPEs were prepared by the *in situ* plating of a Bi film from a $Bi^{3+}$ plating solution.

### 2.5. Sample preparation

Water samples for analysis were prepared by diluting 1.0 mL of tap water with 4.0 mL of supporting electrolyte. Additionally, sea bass fish and undulated surf clam samples were also investigated by mincing the tissue into small pieces and then grinding for a few minutes in a blender machine. After that, known amounts of $Cd^{2+}$ and $Pb^{2+}$ were spiked into a portion of the homogenized sample tissue. Then, 1.0 mL of 13.42 mol $L^{-1}$ $HNO_3$ and 2.0 mL of 11.87 mol $L^{-1}$ $HClO_4$ were added to 1.0 g of this sample homogenate [39], and the sample was heated at 100 °C for 5 h. Next, the solid residue was filtered with filter paper, and the resulting solution was clear. The pH was then adjusted with NaOH and HCl close to pH of the supporting electrolyte before being diluted with the supporting electrolyte to a final volume of

25 mL. The recovery and precision of the extraction method were evaluated by the calibration method for the analysis of water samples following spiking with both metal ions at final concentrations of 7 or 20 μg $L^{-1}$ each. The complex matrix samples (sea bass fish tissues and undulated surf clam) were evaluated after spiking with both metal ions at 25 and 125 mg $kg^{-1}$ prior to extraction by the standard addition method.

## 3. Results and discussion

### 3.1. Structural characterization of graphene and graphite

The Fourier transform infrared (FT-IR) spectra of the as-used graphite and graphene samples are shown in Fig. 1. The spectra of graphite and graphene showed similar band positions, except that the transmission band of graphite exhibited much stronger bands for the O–H (3400 $cm^{-1}$), the C═O (1736 and 1641 $cm^{-1}$) and the C–O groups (1473 to 1379 $cm^{-1}$) compared to graphene [14,40–43]. Thus, the oxygen group was observed to be at a much higher density on the graphite than on the graphene. Therefore, a lower background current might be obtained from the graphene, while the oxide groups on the graphite electrode surface would most likely decrease the sensitivity of the analyte peak during electrochemical detection.

### 3.2. Optimization of the parameters for the GCPE measurement of $Pb^{2+}$ and $Cd^{2+}$ levels

The key factors that influence the performance of the GCPE electrode were evaluated as detailed below as a sequential univariate approach to optimize the Bi-GCPE-based electrode for the simultaneous measurement of the $Cd^{2+}$ and $Pb^{2+}$ ion levels. Because a univariate approach assumes that all of the evaluated factors are independent (which was not established), we therefore refer to these steps as "optimizations" in this manuscript to reflect the limited evaluated range of each variable. Note that for all of these optimization stages (Sections 3.2.1–3.2.3 and 3.3), a 10 μg $L^{-1}$ solution of $Cd^{2+}$ and $Pb^{2+}$ was used.

#### 3.2.1. The graphene and graphite mass ratio

The amount of graphene that is mixed with the graphite powder during the GCPE fabrication affects the electrical conductivity [38,44]. Thus, the effect of the weight fraction of graphene in the GCPE was evaluated from 0.5 to 8.0 mg of graphene at a constant weight (150.0 mg) of graphite nanopowder.

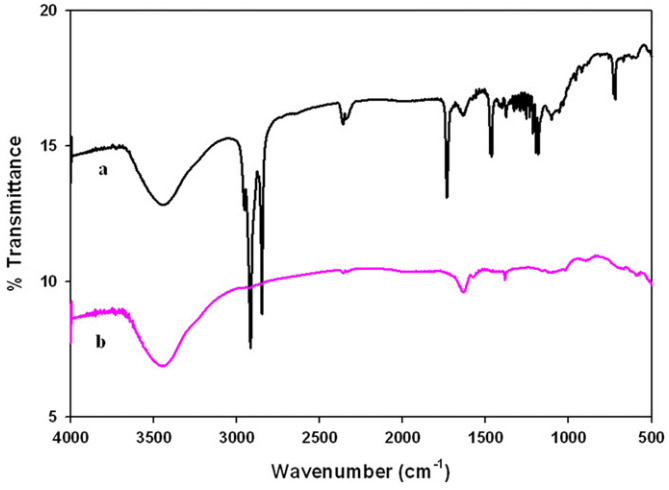


**Fig. 1.** FT-IR spectrum of the as-used (a) graphite and (b) graphene samples.

The electrochemical responses of the $Cd^{2+}$ and $Pb^{2+}$ solutions were used to investigate the electrical conductivity of the different inclusion amounts of graphene in the CPE using 0.1 M HCl as the electrolyte, a deposition potential of −1.25 V, a SW frequency of 50 Hz and a step potential of 0.01 V. The anodic peak current

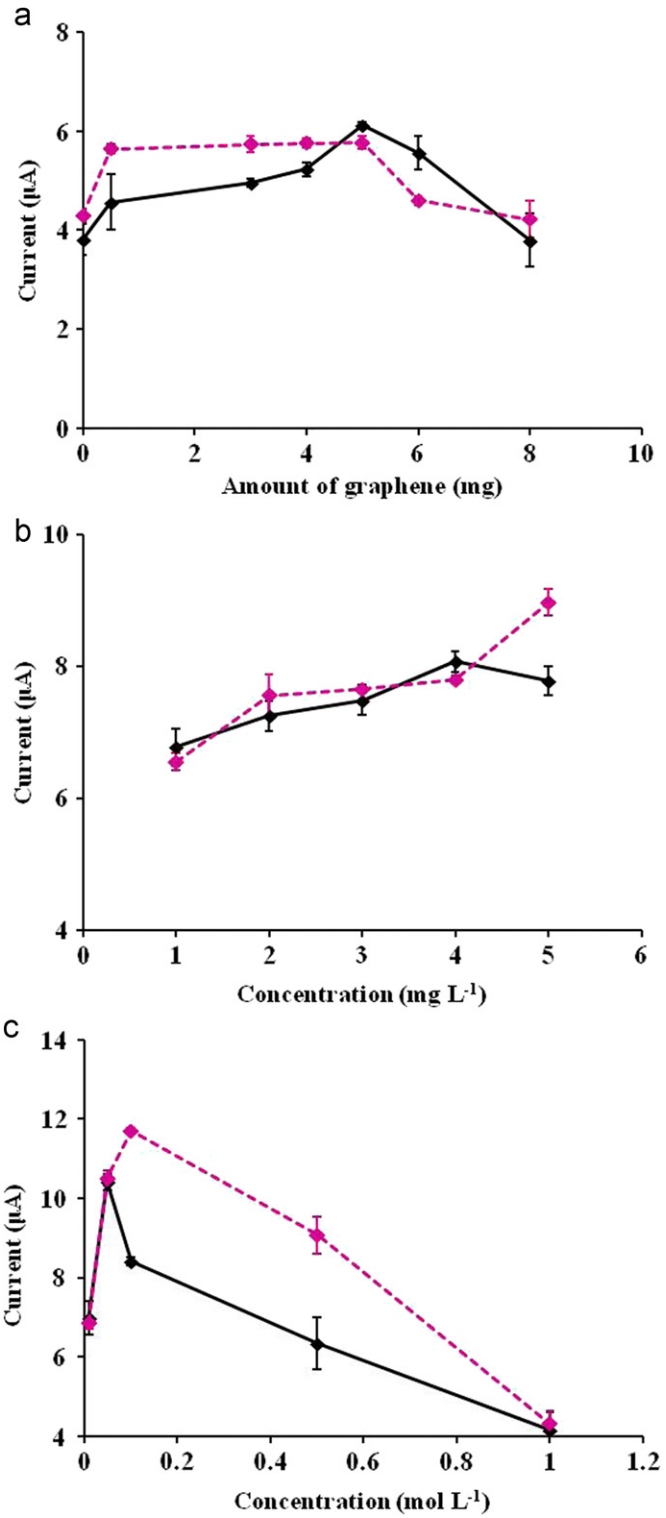


**Fig. 2.** Effect of the (a) graphene:graphite mass ratio, (b) $Bi^{3+}$ concentration in the plating solution, and (c) HCl concentration in the electrolyte solution on the anodic current that was obtained from a 10 μg $L^{-1}$ solution of $Cd^{2+}$ (dashed line) or $Pb^{2+}$ (solid line). The data are shown as the mean ± SD and are derived from four independent repeats.

responses of $Cd^{2+}$ and $Pb^{2+}$ were both higher with the GCPE than with the CPE, and they varied slightly with different graphene:-graphite mass ratios in the GCPE, with an optimal ratio of graphene:graphite of 5.0:150 (w/w) for both $Cd^{2+}$ and $Pb^{2+}$ ions (Fig. 2a). At higher graphene levels a decrease in the anodic peak current signals for both $Cd^{2+}$ and $Pb^{2+}$ was observed. Thus, to obtain the best electrochemical responses, the amount of graphene was chosen at 5.0 mg per 150.0 mg of graphite for all further work.

### 3.2.2. The optimal $Bi^{3+}$ concentration used to modify the GCPE

The coating of electrodes with a Bi film is a well-known method that is used to prevent the electrode surface from degradation by chlorine gas in the supporting electrolyte (HCl) during oxidation, which results in a more reproducible peak current [45]. Therefore, a Bi film was selected to modify the GCPEs in this work. The Bi film thickness on the GCPE was first optimized because the diffusion process of the analyte onto the electrode surface is reported to be influenced by the film thickness [46]. To obtain a satisfactory mechanical film stability and current signal, the influence of the $Bi^{3+}$ ion concentration in the plating solution was evaluated from 1.0 to 5.0 mg $L^{-1}$ for a fixed plating time, and the resulting Bi-GCPEs were evaluated using a deposition potential of −1.25 V, a SW frequency of 50 Hz and a step potential of 0.01 V (Fig. 2b). The mean anodic peak current height for the 10 μg $L^{-1}$ $Cd^{2+}$ solution increased as the $Bi^{3+}$ concentration in the plating solution increased up to 4.0 mg $L^{-1}$ and then decreased at 5.0 mg $L^{-1}$, whereas the mean anodic peak current height for the 10 μg $L^{-1}$ $Pb^{2+}$ solution continuously increased and was maximal at 5.0 mg $L^{-1}$ (the highest tested concentration). The high concentration of the $Bi^{3+}$ solution may cause different forms of Cd–Bi and Pb–Bi intermetallic compounds that result in the partial or full dissociation of metal complex compounds during the stripping step. This phenomenon is likely to be the mass transfer limitation of $Cd^{2+}$ diffusing out of the film during the stripping step, whereas $Pb^{2+}$ continued to diffuse out. Therefore, an optimum concentration of 4.0 mg $L^{-1}$ for the $Bi^{3+}$ plating solution was chosen for all further works as a compromise between the best sensitivity for both $Cd^{2+}$ and $Pb^{2+}$ detection and the minimum measurement error.

### 3.2.3. The influence of HCl concentration in the electrolyte

HCl has been widely recommended as the electrolyte solution for the determination of several metals by anodic stripping voltammetry (ASV) in flow systems. HCl has previously been shown to be the most suitable electrolyte for the determination of $Cd^{2+}$ and $Pb^{2+}$ levels using a SIA–SWASV system [47]. In addition, the use of HCl as the electrolyte is convenient because the same acid is typically used to dissolve the residues after the digestion process during the sample preparation. Therefore, we selected HCl as the supporting electrolyte and evaluated the optimal concentration between 0.01 and 1.0 mol $L^{-1}$ (Fig. 2c), using the Bi-GCPE (as optimized from Sections 3.2.1 and 3.2.2), a deposition potential of −1.25 V, a SW frequency of 50 Hz and a step potential of 0.01 V. The maximum anodic peak current was achieved at a concentration of 0.05 and 0.01 mol $L^{-1}$ HCl for $Cd^{2+}$ and $Pb^{2+}$, respectively, which decreased sharply thereafter with increasing HCl concentrations above 0.05 mol $L^{-1}$. However, because the sensitivity of $Pb^{2+}$ (anodic peak current) decreased

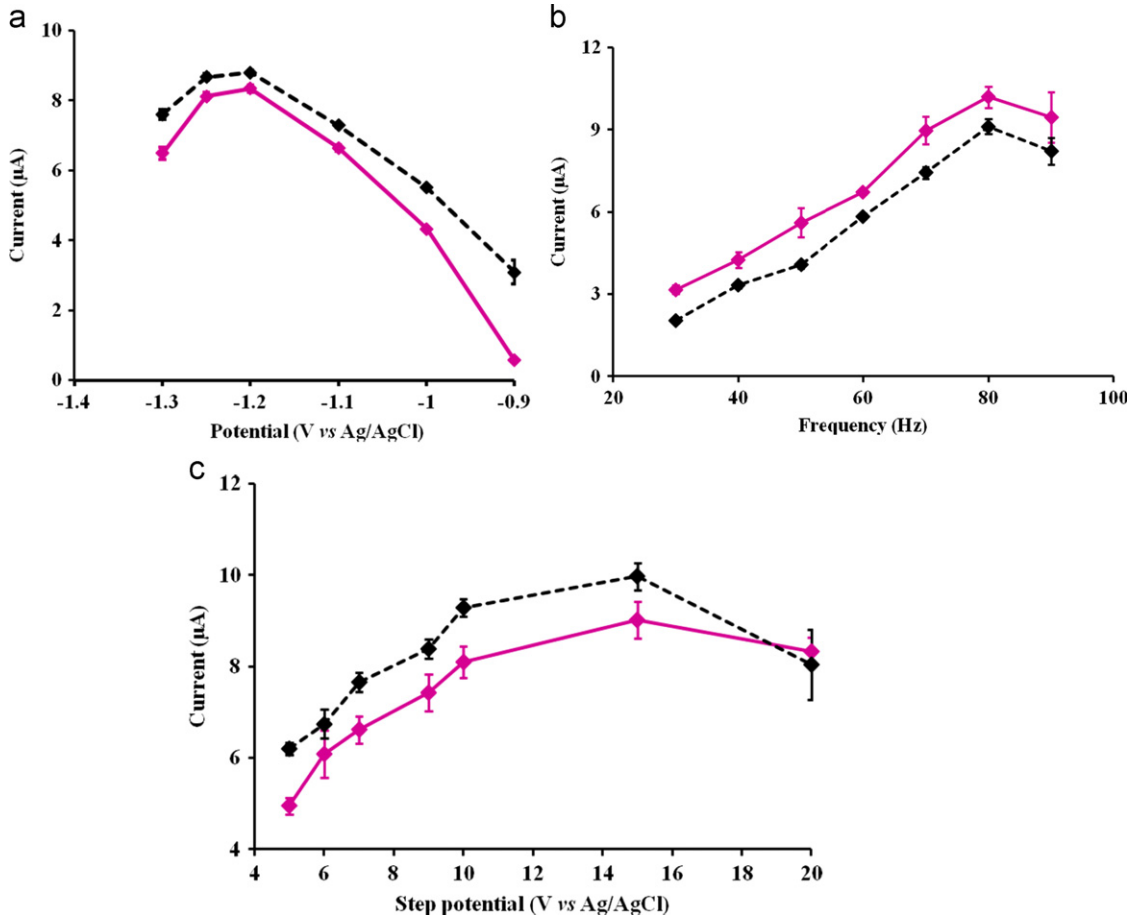


**Fig. 3.** Influence of square wave (SW) parameters on the anodic peak current obtained from a 10 μg $L^{-1}$ solution of $Cd^{2+}$ (dashed line) or $Pb^{2+}$ (solid line) as a function of the (a) deposition potential, (b) SW frequency, and (c) step potential. The data are shown as the mean ± SD and are derived from four independent repeats.

at 0.1 mol $L^{-1}$, an HCl concentration of 0.05 mol $L^{-1}$ was chosen as the optimum electrolyte concentration for use in the subsequent work.

### 3.3. Optimization of Bi-GCPE electrochemical parameters

The current signal that is obtained in SIA–SWASV is dependent on the operational parameters, including the deposition potential, SW frequency and the step potential. Therefore, these three parameters were optimized next using the optimized Bi-GCPE and 0.05 M HCl as the electrolyte. First, the influence of the deposition potential, or accumulation potential, was evaluated from −1.3 to −0.9 V with a SW frequency of 50 Hz and a step potential of 0.01 V (Fig. 3a). For both $Cd^{2+}$ and $Pb^{2+}$ detection, a maximum anodic peak current was observed with a depositional potential of −1.2 V *vs.* Ag/AgCl. Higher or lower deposition potentials resulted in a lower current and a poor standard deviation (worse reproducibility). Thus, a deposition potential of −1.2 V *vs.* Ag/AgCl was selected.

The SW frequency is related to the scan rate of the method [46,48] and was evaluated from 30 to 90 Hz using a deposition potential of −1.2 V *vs.* Ag/AgCl and a step potential of 0.01 V (Fig. 3b). The anodic peak currents for both $Cd^{2+}$ and $Pb^{2+}$ increased as the SW frequency increased up to 80 Hz and then decreased with a larger standard error at 90 Hz. Thus, a SW frequency of 80 Hz was selected.

Finally, the effect of varying the step potential was investigated from 5.0 to 20 mV, with a depositional potential of −1.2 V *vs.* Ag/AgCl and a SW frequency of 80 Hz. The analytical signal was found to increase as the step potential was increased up to 15 mV for both $Cd^{2+}$ and $Pb^{2+}$ detection and then decreased at higher step potential values (Fig. 3c). Thus, a step potential of 15 mV was selected for use in all subsequent experiments.

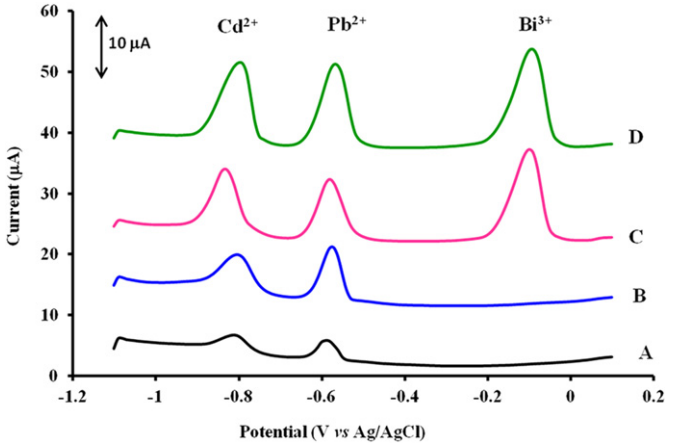


**Fig. 4.** Representative (from four independent samples) voltammograms of 10 µg $L^{-1}$ solutions of $Cd^{2+}$ and $Pb^{2+}$ that were obtained from (a) CPE, (b) GCPE, (c) Bi-CPE, and (d) Bi-GCPE.

### 3.4. Electrochemical characteristics of the electrode

The comparison between the voltammograms of the electrolyte solution containing 10 µg $L^{-1}$ of $Cd^{2+}$ and $Pb^{2+}$ that were obtained with the Bi-GCPE, GCPE, Bi-CPE and CPE under the optimized conditions is shown in Fig. 4. The anodic peak currents of both metal ions exhibited well-defined peaks, with the highest peak current being observed with the Bi-GCPE, followed by that

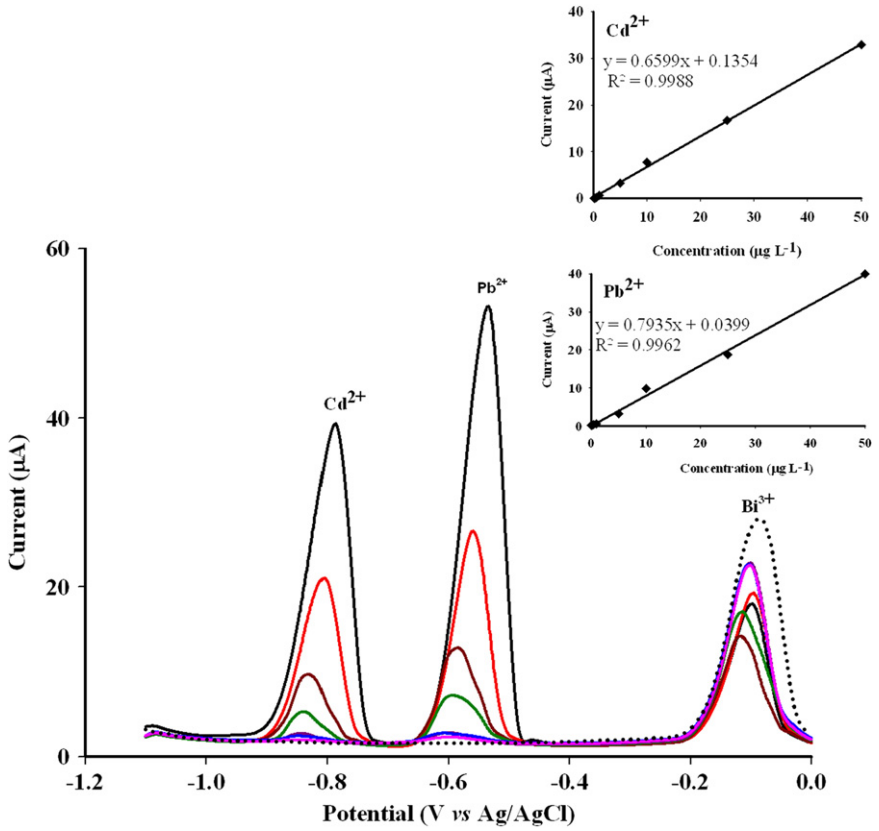


**Fig. 5.** Representative (from four independent replicates) voltammograms of $Cd^{2+}$ and $Pb^{2+}$ at different concentrations measured by SWASV with Bi-GCPE under the optimized conditions and (inset) the calibration plot between the anodic current peak height and the heavy metal ion concentration.

from the Bi-CPE and then GCPE and CPE. These data illustrate the importance of the Bi film and also suggest that the high conductivity, surface area and the electron-transfer rate between the analyte molecule and the electrode surface of graphene could enhance the sensitivity. Thus, for the determination of $Cd^{2+}$ and $Pb^{2+}$ by an automated flow system, the Bi-GCPE appears to be more sensitive than the other types of carbon electrodes that have previously been applied in flow systems.

### 3.5. Analytical parameters

Under the optimized Bi-GCPE composition (Sections 3.2.1 and 3.2.2) and electrochemical analytical conditions (Sections 3.2.3 and 3.3), the calibration data of the $Cd^{2+}$ and $Pb^{2+}$ anodic peak current that were obtained at different metal ion concentrations (0.1–100 μg $L^{-1}$ for both metal ions) was collected (Fig. 5). From the results, the stripping peak currents were found to be proportional to the concentration of $Cd^{2+}$ and $Pb^{2+}$ within the range of 0.1–50.0 μg $L^{-1}$, with good linear regression correlation coefficients ($r^2$) of $>0.995$. The LOD, evaluated as the concentration that gave a response equivalent to three times the SD of the blank ($n=10$), the limit of quantification (LOQ), evaluated as the concentration that gives a response equivalent to ten times the SD of the blank, and the precision of the procedure, expressed by the relative standard deviation for three measurements of each metal ion, are summarized in Table 1. We conclude that the Bi-GCPE under these optimized automated flow conditions gives a satisfactorily high sensitivity, an acceptable level of precision and a rapid analysis.

### 3.6. Applications

To evaluate the application of this Bi-GCPE, it was applied under these optimized conditions for the determination of $Cd^{2+}$ and $Pb^{2+}$ levels in both non-complicated (tap water) and complicated (sea bass fish and undulated surf clams) matrix samples.

**Table 1**
The analytical performance of $Cd^{2+}$ and $Pb^{2+}$ determination by SIA–SWASV with the Bi-GCPE under the optimized conditions.

| Metal ion | Linearity range (μg $L^{-1}$) | $r^2$ | LOD (μg $L^{-1}$) | LOQ (μg $L^{-1}$) |
|---|---|---|---|---|
| $Cd^{2+}$ | 0.1–50.0 | 0.9988 | 0.07 | 0.23 |
| $Pb^{2+}$ | 0.1–50.0 | 0.9962 | 0.04 | 0.15 |

#### 3.6.1. Non-complicated matrix: tap water sample

The concentrations of $Cd^{2+}$ and $Pb^{2+}$ in the tap water sample were evaluated by the calibration method without pretreatment or filtration. No signal peak current of $Cd^{2+}$ and $Pb^{2+}$ was obtained in the unspiked tap water sample. The average concentrations of $Cd^{2+}$ and $Pb^{2+}$ in the spiked tap water samples were found to be slightly lower than the spiked amount, with a 79–86% and 87–92% recovery when spiked at 7.0 and 20.0 μg $L^{-1}$, respectively (Table 2). However, the standard deviations were relatively small, which suggested a reasonable level of reproducibility.

#### 3.6.2. Complicated matrix: sea bass fish and undulated surf clams

After the sample preparation, the ability to detect and quantify trace levels of $Cd^{2+}$ and $Pb^{2+}$ ions in sea bass fish and undulated surf clam tissues under the optimized conditions were evaluated by the standard addition method, which is used for samples when matrix effects could influence the analytical method. The accuracy of the SIA–SWASV procedure with the Bi-GCPE was evaluated by the recovery assay using $Cd^{2+}$ and $Pb^{2+}$ additions (spiking levels) of 25 and 125 mg $kg^{-1}$ into the sea bass fish and undulated surf clam tissues before starting the extraction process. The voltammetric curves that were obtained are presented in Fig. 6, and the obtained results in these heavy metal ion determinations are summarized in Table 2. The shapes and widths of the peaks were

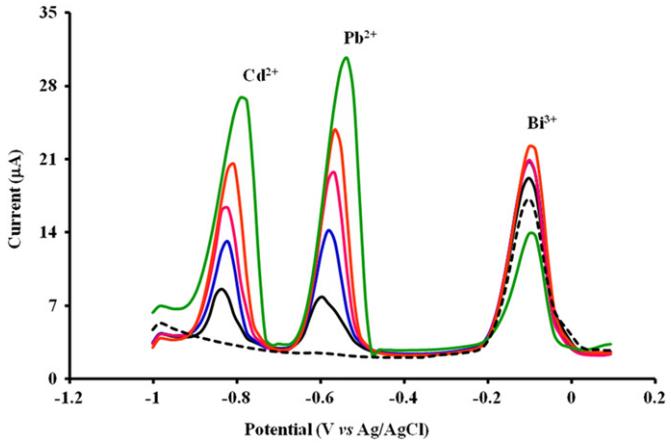


**Fig. 6.** Representative (from four independent samples) voltammograms of $Cd^{2+}$ and $Pb^{2+}$ in undulated surf clam tissues spiked with 125 μg $kg^{-1}$ of $Cd^{2+}$ and $Pb^{2+}$, including the sample blank solution after changing the initial scan. Also shown is the voltammogram for $Bi^{3+}$ from the Bi-GCPE.

**Table 2**
Determination of (spiked) $Cd^{2+}$ and $Pb^{2+}$ levels in a non-complicated (tap water) or complicated (sea bass fish and undulated surf clam tissues) matrix with the Bi-GCPE under SWASV ($n=4$).

| | Spiked level (μg $L^{-1}$) | Found ± SD (μg $L^{-1}$) | | Recovery ± SD (%) | |
|---|---|---|---|---|---|
| | | $Cd^{2+}$ | $Pb^{2+}$ | $Cd^{2+}$ | $Pb^{2+}$ |
| Non-complicated matrix sample | | | | | |
| Tap water | 0 | ND | ND | ND | ND |
| | 7 | 6.13 ± 0.06 | 6.11 ± 0.03 | 87.6 ± 0.82 | 88.1 ± 0.44 |
| | 20 | 18.4 ± 0.20 | 19.3 ± 0.30 | 91.8 ± 1.0 | 96.3 ± 1.4 |
| Complicated matrix sample | | | | | |
| Sea bass fish | 0 | ND | ND | ND | ND |
| | 25 | 25.25 ± 0.05 | 27.50 ± 0.05 | 101.0 ± 5.5 | 110.0 ± 5.0 |
| | 125 | 76.25 ± 0.01 | 81.5 ± 0.06 | 61.0 ± 0.2 | 65.2 ± 1.1 |
| Undulated surf clams tissue | 0 | ND | ND | ND | ND |
| | 25 | 28.13 ± 0.02 | 28.75 ± 0.01 | 112.5 ± 1.6 | 115.0 ± 1.2 |
| | 125 | 147.8 ± 0.11 | 135.3 ± 0.30 | 118.2 ± 2.3 | 108.2 ± 6.0 |

ND = not detectable.

**Table 3**
Concentration of $Cd^{2+}$ and $Pb^{2+}$ in complicated matrix samples (sea bass fish and undulated surf clams) spiked with 250 μg $Kg^{-1}$ of both metal ions found by SIA–SWASV and ICP-OES methods ($n=3$, $P=0.05$, $t_{critical}=4.30$).

| Sample | SIA–SWASV method | | ICP-OES method | | $t_{calulated}$ | |
|---|---|---|---|---|---|---|
| | found ± SD (μg $kg^{-1}$) | | found ± SD (μg $kg^{-1}$) | | | |
| | $Cd^{2+}$ | $Pb^{2+}$ | $Cd^{2+}$ | $Pb^{2+}$ | $Cd^{2+}$ | $Pb^{2+}$ |
| Sea bass fish | 228.3 ± 0.25 | 246.5 ± 0.46 | 267.0 ± 0.25 | 252.8 ± 0.87 | 1.88 | 0.40 |
| Undulated surf clams | 227.5 ± 0.49 | 295.3 ± 0.27 | 251.3 ± 1.63 | 280.5 ± 0.93 | 3.93 | 2.07 |

similar to those that were obtained for the standard solution. However, when the samples contained a low concentration of $Cd^{2+}$ or $Pb^{2+}$, a significant level of interference from the matrix was obtained, and the current peak of $Cd^{2+}$ disappeared (data not shown). This problem was overcome by changing the initial scan during the stripping step to −1.10 V *vs.* Ag/AgCl to improve the resolution of $Cd^{2+}$, as has previously been reported [49]. The current from the matrix diffusion was then eliminated from the voltammograms, and the recovery percentages for both metal ions when spiked at either 25 or 125 mg $Kg^{-1}$ were very satisfactory (Table 2).

Moreover, the method described in this work was compared with the standard ICP-OES method on the complicated matrix (sea bass fish and undulated surf clam) samples spiked with 125.0 and 250.0 mg $kg^{-1}$ of $Cd^{2+}$ and $Pb^{2+}$. At the spiked concentration of 125.0 mg $kg^{-1}$, neither $Cd^{2+}$ nor $Pb^{2+}$ could be detected using the ICP-OES method, but they were detected using the SIA–SWASV method with the Bi-GCPE (Table 2). The concentrations of $Cd^{2+}$ and $Pb^{2+}$ found in the complicated matrix samples after spiking with 250.0 mg $kg^{-1}$ of $Cd^{2+}$ and $Pb^{2+}$ are shown in Table 3. A paired *t*-test at the 95% confidence level was applied, and the $t_{calculated}$ was below $t_{critical}$ (4.30 at 2 degrees of freedom), which suggested no significant difference between the two methods. Therefore, the proposed SIA–SWASV method using a Bi-GCPE is useful for the simultaneous determination of $Cd^{2+}$ and $Pb^{2+}$ in complicated matrix samples.

## 4. Conclusions

A highly enhanced sensing electrode, a Bi-GCPE composite film, was successfully established for the automated simultaneous determination of trace levels of the heavy metal $Cd^{2+}$ and $Pb^{2+}$ ions using SWASV in a SIA system. This report is the first demonstration of the application of a Bi-GCPE to SIA for the SWASV measurement of trace levels of $Cd^{2+}$ and $Pb^{2+}$ in real-world samples. This method can be used for the determination of trace levels of $Cd^{2+}$ and $Pb^{2+}$ in high matrix samples, which was exemplified by sea bass fish and undulated surf clam tissues. It offers the significant advantage of an excellent electrical conductivity and increased surface area from the graphene that was mixed with graphite nanopowder. This use of the graphene composite film electrode in a flow system, combined with a Bi film, enabled the LODs of only 0.07 and 0.04 μg $L^{-1}$ for $Cd^{2+}$ and $Pb^{2+}$, respectively, which are lower than those that were previously obtained by CNT-based electrodes at 0.80 and 0.20 μg $L^{-1}$ for $Cd^{2+}$ and $Pb^{2+}$, respectively [50].

## Acknowledgments

Financial support from the Commission on Higher Education, Ministry of Education, Thailand, under the Higher Educational Strategic Scholarships for Frontier Research Network Project; the Center of Excellence for Petroleum, Petrochemicals and Advanced Materials, the 90th Anniversary of Chulalongkorn University Fund (Ratchadaphiseksomphot Endowment Fund), are gratefully acknowledged. O.C. greatly thanks the Thai Government Stimulus Package 2 (TKK2555), under the Project for Establishment of Comprehensive Center for Innovative Food, Health Products and Agriculture and The National Research University Project of CHE and Ratchadaphiseksomphot Endowment Fund (Project code AM1009I-55). The Publication Counseling Unit (PCU007.2012), is also acknowledged for suggestions and English corrections. We are grateful to the Department of Chemistry, Faculty of Science, Chulalongkorn University, for providing chemicals and laboratory facilities.

## References

[1] D.C. Marcano, D.V. Kosynkin, J.M. Berlin, A. Sinitskii, Z. Sun, A. Slesarev, L.B. Alemany, W. Lu, J.M. Tour, ACS Nano 4 (2010) 4806–4814.
[2] G. Lu, S. Mao, S. Park, R. Ruoff, J. Chen, Nano Res. 2 (2009) 192–200.
[3] M.M. Gudarzi, F. Sharif, J. Colloid Interface Sci. 349 (2010) 63–69.
[4] M. Liang, B. Luo, L. Zhi, Int. J. Energy Res. 33 (2009) 1161–1170.
[5] M. Pumera, Chem. Rec. 9 (2009) 211–223.
[6] M. Winter, J.O. Besenhard, M.E. Spahr, P. Novák, Adv. Mater. 10 (1998) 725–763.
[7] P. Guo, H. Song, X. Chen, Electrochem. Commun. 11 (2009) 1320–1324.
[8] T. Wei, F. Wang, J. Yan, J. Cheng, Z. Fan, H. Song, J. Electroanal. Chem. 653 (2011) 45–49.
[9] J.J. Yoo, K. Balakrishnan, J. Huang, V. Meunier, B.G. Sumpter, A. Srivastava, M. Conway, A.L. Mohana Reddy, J. Yu, R. Vajtai, P.M. Ajayan, Nano Lett. 11 (2011) 1423–1427.
[10] K.-S. Kim, S.-J. Park, Electrochim. Acta 56 (2011) 6547–6553.
[11] M. Pumera, A. Ambrosi, A. Bonanni, E.L.K. Chng, H.L. Poh, TrAC Trends Anal. Chem. 29 (2010) 954–965.
[12] W. Li, C. Tan, M.A. Lowe, H.C.D. Abruna, D.C. Ralph, ACS Nano 5 (2011) 2264–2270.
[13] N.G. Shang, P. Papakonstantinou, M. McMullan, M. Chu, A. Stamboulis, A. Potenza, S.S. Dhesi, H. Marchetto, Adv. Funct. Mater. 18 (2008) 3506–3514.
[14] C.M. Willemse, K. Tlhomelang, N. Jahed, P.G. Baker, E.I. Iwuoha, Sensors 11 (2011) 3970–3987.
[15] J. Gong, T. Zhou, D. Song, L. Zhang, Sensors Actuators B: Chem. 150 (2010) 491–497.
[16] K. Ku, B. Kim, H. Chung, W. Kim, Synth. Met. 160 (2010) 2613–2617.
[17] Y. Song, Z. He, H. Zhu, H. Hou, L. Wang, Electrochim. Acta 58 (2011) 757–763.
[18] X.-W. Liu, J.-J. Mao, P.-D. Liu, X.-W. Wei, Carbon 49 (2011) 477–483.
[19] C.-T. Hsieh, J.-M. Wei, J.-S. Lin, W.-Y. Chen, Catal. Commun. 16 (2011) 220–224.
[20] S. Wu, X. Lan, L. Cui, L. Zhang, S. Tao, H. Wang, M. Han, Z. Liu, C. Meng, Anal. Chim. Acta 699 (2011) 170–176.
[21] M.B. Zubero, J.J. Aurrekoetxea, J.M. Ibarluzea, M.J. Arenaza, C. Rodríguez, J.R. Sáenz, Sci. Total Environ. 408 (2010) 4468–4474.
[22] G. Marino, M.F. Bergamini, M.F.S. Teixeira, E.T.G. Cavalheiro, Talanta 59 (2003) 1021–1028.
[23] Y. Ren, Z. Zhang, Y. Ren, W. Li, M. Wang, G. Xu, Talanta 44 (1997) 1823–1831.
[24] P. Yáñez-Sedeño, J.M. Pingarrón, J. Riu, F.X. Rius, TrAC Trends Anal. Chem. 29 (2010) 939–953.
[25] T. Marek, TrAC Trends Anal. Chem. 25 (2006) 480–489.
[26] J. Li, S. Guo, Y. Zhai, E. Wang, Anal. Chim. Acta 649 (2009) 196–201.
[27] B. Wang, Y.-h. Chang, L.-j. Zhi, New Carbon Mater. 26 (2011) 31–35.
[28] B.G. Choi, J. Im, H.S. Kim, H. Park, Electrochim. Acta 56 (2011) 9721–9726.
[29] G.H. Hwang, W.K. Han, J.S. Park, S.G. Kang, Talanta 76 (2008) 301–308.
[30] J.C. Quintana, F. Arduini, A. Amine, F. Punzo, G.L. Destri, C. Bianchini, D. Zane, A. Curulli, G. Palleschi, D. Moscone, Anal. Chim. Acta 707 (2011) 171–177.
[31] S.M. Skogvold, Ø. Mikkelsen, J. Electroanal. Chem. 20 (2008) 1738–1747.
[32] D. John F, Surf. Sci. 605 (2011) 1621–1632.

[33] J. Guo, L. Ren, R. Wang, C. Zhang, Y. Yang, T. Liu, Composites, Part B: Eng. 42 (2011) 2130–2135.
[34] X. Shen, L. Jiang, Z. Ji, J. Wu, H. Zhou, G. Zhu, J. Colloid Interface Sci. 354 (2011) 493–497.
[35] Wei Yu, Huaqing Xie, Xinwei Wang, X. Wang, Nanoscale Res. Lett. 6 (2011) 1–7.
[36] N.-W. Pu, C.-A. Wang, Y.-M. Liu, Y. Sung, D.-S. Wang, M.-D. Ger, J. Taiwan Inst. Chem. Eng. 43 (2011) 140–146.
[37] P.Mohammad Hadi, Electrochem. Commun. 13 (2011) 366–369.
[38] F. Li, J. Li, Y. Feng, L. Yang, Z. Du, Sensors Actuators B: Chem. 157 (2011) 110–114.
[39] V. Meucci, S. Laschi, M. Minunni, C. Pretti, L. Intorre, G. Soldani, M. Mascini, Talanta 77 (2009) 1143–1148.
[40] H.-L. Guo, X.-F. Wang, Q.-Y. Qian, F.-B. Wang, X.-H. Xia, ACS Nano 3 (2009) 2653–2659.
[41] Y. Harima, S. Setodoi, I. Imae, K. Komaguchi, Y. Ooyama, J. Ohshita, H. Mizota, J. Yano, Electrochim. Acta 56 (2011) 5363–5368.
[42] S. Chandra, S. Sahu, P. Pramanik, Mater. Sci. Eng. B 167 (2010) 133–136.
[43] Y. Si, E.T. Samulski, Nano Lett. 8 (2008) 1679–1682.
[44] T. Battumur, S.H. Mujawar, Q.T. Truong, S.B. Ambade, D.S. Lee, W. Lee, S.-H. Han, S.-H. Lee, Curr. Appl. Phys. (2011) 1–5.
[45] E.C. Juan-Sánchez, P. Corredor, J. Ágreda, Port. Electrochim. Acta 29 (2011) 197–210.
[46] J.-M. Zen, Y.-S. Ting, Anal. Chim. Acta 342 (1997) 175–180.
[47] S. Chuanuwatanakul, W. Dungchai, O. Chailapakul, S. Motomizu, Anal. Sci. 24 (2008) 589–594.
[48] M. Chojak Halseid, Z. Jusys, R.J. Behm, J. Electroanal. Chem. 644 (2010) 103–109.
[49] R.E.C. Vedhi, H. Gurumallesh-Prabu, P. Manisankar, Int. J. Electrochem. Sci. 3 (2008) 509–518.
[50] U. Injang, P. Noyrod, W. Siangproh, W. Dungchai, S. Motomizu, O. Chailapakul, Anal. Chim. Acta 668 (2010) 54–60.